Nano-composite Fibers Based on Poly(p-benzamide)-Montmorillonite

Enrico Marsano, Francesco Azzurri, Paola Corsini*

Summary: Nano-composites fibers made of poly(p-benzamide) (PBA), a rigid liquid crystalline polymer, and an inorganic nano-filler, montmorrilonite (MMT), were prepared by a wet spin process. Dimethylacetamide-3% (w/w) LiCl was used as a solvent. Polymer concentration, $Cp = 6.5\%$ (w/w), was maintained as high as possible, but lower than the critical concentration for the appearance of a liquid crystalline phase, $Cp' = 6.7\%$. MMT dispersed in PBA solution was 2.6–5.0% (w/w) with respect to PBA. The Polymer-MMT solutions show a liquid crystalline phase at polymeric concentration above 6.7% and they show by a high metastability and a slow phase separation.The PBA-MMT solutions show good spinnability and fibers are characterized by a significant increasing in modulus and breaking strength. WAXD and TEM analyses suggest that partially intercalated PBA/MMT nano-composite fibers have been obtained.

Keywords: Fiber; liquid crystal; nanocomposite; polyamide; wet-spinning

Introduction

Polymer systems are widely used due to their unique attributes: ease production, light weight and ductile nature. However polymers have low modulus and strength compared to metals and ceramics. One way to improve mechanical properties is to reinforce them with inclusions (fibers, whiskers, platelets or particles). Traditionally, composites were reinforced with micron-sized inclusions, while processing techniques have recently been developed towards nano-scale size, that have at least one dimension in the range of 1–100 nm.[1–5] Some nano-fillers are based on tiny platelets of a special type of modified clay surface called montmorillonite (MMT), that are a naturally occurring raw material found in abundance. This montmorillonite is a family of phyllosilicates that comprises two tetrahedral silica thin layers with a central octahedral sheet of magnesia. Isomorphic substitution within the layers gives a hydrophilic nature. The clays are mined and then processed into commercially available end products. Among various organic compounds, ammonium cations are typically used to treat this clay and they are used to minimize the attractive forces between the agglomerated clay platelets. The typical agglomerated platelets are separated by approximately 1nm. The cation treatment presumably acts on the platelets to separate them. The separation distance will depend on cation molecule size and a distance of about 2 nm can be achieved. This intercalation process opens the spacing between the platelets enough so that the monomer or polymer can penetrate between platelet layers. Without this, the reinforcing nature of the platelets will not occur. Although current micromechanic theories for micron size reinforcement rely on the idea that the effective properties of composite materials

Dipartimento di Chimica e Chimica Industriale, Università di Genova, Via Dodecaneso 31-16146 Genova, Italy
Phone - fax: +390103538727
E-mail: marsano@unige.it

are independent of inclusion size, it may not be true for nano-composite systems.[6]

Experiments have clearly shown that nano-scale reinforcements lead to new phenomena which contribute to material properties, such as the in influencing the crystallization process. In particular, matrix polymer tends to crystallize around dispersed particles, increasing flexural modulus, heat distortion temperature and barrier properties.[6]

It should be noticed that the most publications about polymer nanocomposites concern their film materials, and only a few papers are related to nanocomposite fibers prepared by melt spinning.[7–12] Besides, the wet spinning process is seldom used to produce nanocomposite fibers[13], but this method could be interesting because it offers the possibility to apply the solution intercalation technique.

In this work an aromatic lyotropic polyamide Poly(p-benzamide) (PBA) was used in the solvent Dimethylacetamide (DMAc)–LiCl. The solutions, then, were blended with nano-filler MMT, and were spun into the nanocomposite fibers via wet spinning technique. The mechanical property as well as morphology of the PBA-MMT nanocomposite fibers were investigated.

Experimental

Material and Method

PBA Synthesis

Samples of PBA were prepared from p-amino benzoic acid following Yamazaki's method.[14] Synthesis conditions were: $T = 100\,^{\circ}C$ and polymerization time was about 2.5 h.

Viscometry

The molecular weight was determined from intrinsic viscosity in 96% H_2SO_4 at $25\,^{\circ}C$ using the relationship $[\eta] = 1.9 \times 10^{-7}\, M_v^{1.7}$.[15]

Nano Filler

Organophilic montmorillonite under the trade name of Cloisite from Southern Clay Products Inc. USA, with different type of alkylammonium ions were considered in this study: Cloisite 10A is organically modified with dimethyl benzyl hydrogenated tallow quaternary ammonium cations (MMT-10A); Cloisite 20A is organically modified with dimethyl dehydrogenated tallow quaternary ammonium cations (MMT-20A); Cloisite 30B is organically modified with methyl tallow bis-2-hydroxyethyl quaternary ammonium cations (MMT-30B).

Dope Preparation

Concentrated solutions for spinning were prepared by adding DMAc/3% (w/w) LiCl as solvent to polymer, stirring at a low speed at room temperature for about a day. In some samples, MMT was directly dispersed in PBA solution. The total amount of MMT was added in three times, and after each step the solution were stirred vigorously for half a day. Prior to spinning, dopes were filtered through poly(propylene) gauze.

Phase Behaviour

The critical concentration, Cp′, at which the anisotropic phase appears, was determined using optical microscopy Polyvar Pol, supported by reological measurements obtained by using a Brookfield viscometer (LVDV-II+ with SC4-8R(P) chamber and SC4-16 spindle). Measurements were performed with a 4.2 ml dope volume at room temperature at different shear rate.

Spinning

Fibers were obtained by using the spinning line described in a previous paper.[16] The extrusion rate at 100 μm spinnerette was fixed at $V_o = 8$ m/min, corresponding to a shear rate of 10600 s^{-1}, with a spinning temperature of $25\,^{\circ}C$. Fibers were collected using "as spun" conditions (no stretch applied during coagulation, $V_l/V_f = 1$) and under stretching ratio ($V_l/V_f = 2$) where V_f is fiber velocity at the spinnerette hole without any stretch and V_l is the take-up speed. Water at room temperature was used as coagulation bath and washing

solvent. Fibers were further washed for about 48 hours to eliminate all LiCl salt.

Fiber Characterization

Stress-strain measurements were made with an Instron dynamometer mod. 5500. Elastic modulus (E), strength (σ_b) and elongation (ε_b) at break are averaged for at least 10 determinations, using monofilaments. The errors values were estimated are being 1%, on E and σ_b and 15% on ε_b values. Measurements were performed using a 50mm gauge distance and $1.7 \cdot 10^{-3}$ s^{-1} deformation rate.

X-ray

The interlayer spacing of the MMT in the PBA nano-composite fibers was examined by wide-angle X-ray diffraction. Measurements were obtained at 20 °C using a Philips 1861 diffractometer equipped with Cu Kα radiation, $\alpha = 0.154$ nm. MMT was analysed after a treatment in a DMAc-3% (w/w) LiCl solution for at least 5–6 hours, in order to reproduce the solution condition. Fibers were cut, mixed and pressed obtaining a random panel to be measured by X-ray diffraction.

TEM

Transmission electron microscopy experiments were performed using a JEM 2010 transmission electron microscope, in order to directly observe the layer of nanocomposites. Ultrathin sections of bulk samples were produced at −100 °C using a Leica Ultracut UCT with EMFCS cryoattachment. The sections were floated off diamond knife and transferred to grids. To measure the thickness of the layers of MMT in the fibers an image management program ''ImageJ'' was used. About sixty layers thickness measurements were taken for each fibers, homogenously along the sections, in order to obtain their frequency distribution.

TGA

Thermogravimetric analysis was conducted in flowing oxygen (30 cm^3 min^{-1}) from 50 to 900 °C at a heating rate of 10 °C min^{-1} using a Perkin–Elmer TGA 7.

Results and Discussion

The first step of this work was focused on the choice of MMT that showed the greater swelling degree in DMAc. According to the procedure suggested by Duchet[17] 5 g of MMT were introduced into a graduated test tube containing 100 ml of solvent. Without any mixing, the system was allowed to rest and the sedimented volume of swollen nanoclay was measured after 24 h.

In order to compare the different degree of swelling the factor S, defined as $S = (V_s - V_o)/V_o$ where V_s is the final slurry volume and V_o the dry powder volume, was evaluated. The measures were realized in DMAc with different amount of LiCl. All the organo-clay dispersion in DMAc resulted in a slightly turbid suspension and MMT-30B showed the greater swelling degree, $S = 2.4$. A continuous decrease of the swelling was observed as the amount of LiCl increased. A final swelling degree of 0.8 was observed in DMAc containing 3% (w/w) LiCl. Similar results were obtained with other two nanoclay: MMT-20A and MMT-10A in DMAc 3% (w/w) LiCl.

To verify the influence of ion Li^+ on the lamellar distances of all used MMT, X-ray analysis were performed on MMT after the dissolution process. The MMT were recovered from the dispersion by centrifugation at 7000 rpm, washed with DMAc to eliminate the excess of LiCl and dried at 120 °C under vacuum for 3 days for a complete removal of DMAc.

X-Ray diffraction patterns of DMAc-LiCl treated MMT showed some differences in the lamellar thickness value respect to the original MMT. All the treated MMT give a similar lamellar distance of about 1.21 nm respect to 1.8 nm observed for the MMT-30B (Figure 1).

This contraction can be correlated to the exchange of the organo-ammonium quaternary ion with the smaller cations Li^+. This means that DMAc-LiCl strongly modify MMT, after the solution treatment the nanofiller can be considered as MMT-Li^+. In the following we used MMT-30B after treatment in DMAc-LiCl.

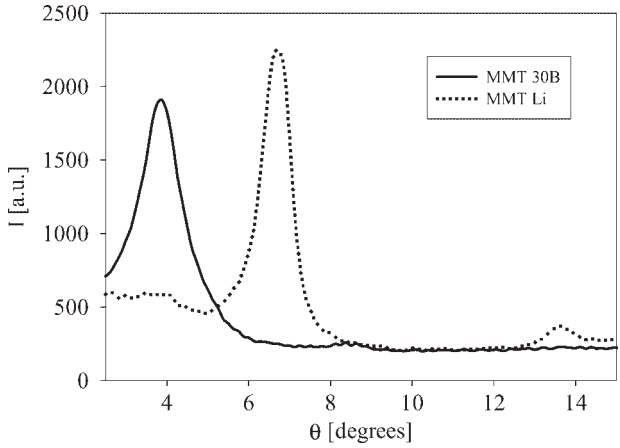

Figure 1.
X-Ray measurement of MMT-30B [solid line] and MMT after treatment with DMAc/3% (w/w) LiCl [dotted line].

PBA is able to give liquid crystalline solutions in DMAc-3% (w/w) LiCl and the phase behaviour was determined by optical microscope analysis and a value of the critical concentration $Cp' = 6.7\%$ (w/w) was found. This value agrees with those reported in literature.[16] Solutions of PBA/DMAc-LiCl/MMT with different PBA concentrations were prepared with 2.6 or 5% (w/w) of MMT with respect to PBA and they were characterized by optical and reological measurements. The optical microphotography, reported in Figure 2 refers to a $C_p = 7\%$ (w/w) solution with 2.6% (w/w) of MMT and the photograph confirms the existence of a liquid crystalline phase. Viscosity vs concentration behaviour extrapolated to zero shear rate is reported in Figure 3, for sample containing 2.6% (w/w) MMT. An increase in viscosity up to a maximum value followed by a sharp decrease, was observed; this behaviour, well known for solution of rigid or semirigid polymers,[18] is correlated to the formation of a mesophase at a concentration near to the maximum values.

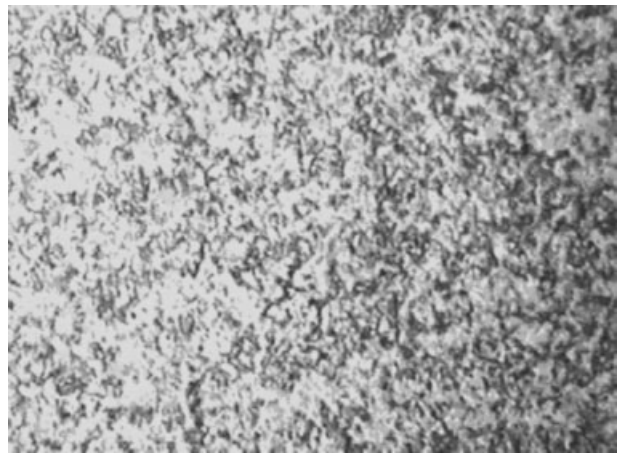

Figure 2.
Photograph, under polarizing microscope, of a liquid crystalline solution composed of: PBA/2.6% (w/w) MMT/DMAc-3% (w/w) LiCl, at overall polymer concentration $Cp = 7\%$ (w/w).

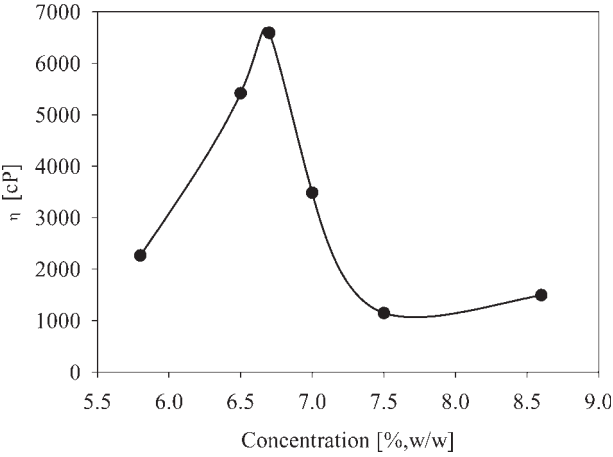

Figure 3.
Viscosity vs concentration behaviour of PBA/2.6%(w/w) MMT solution in DMAc/3%(w/w) LiCl.

It is important to notice that the mesophase appears at the same concentration for PBA/DMAc-LiCl and PBA/DMAc-LiCl/MMT, clearly indicating that the nano-filler has no influence on PBA phase behaviour up to a concentration of 5% (w/w) with respect to PBA.

One of the targets of this work was to achieve fiber starting from dope where there was MMT. Firstly, we noticed that fibers could not be obtained from PBA solution with MMT at a polymer concentration higher than the critical one (Cp′). Since PBA/DMAc-LiCl anisotropic solutions are metastable, as previously reported in literature,[19] the presence of MMT nanoparticles in the solutions increases metastability, and increases the kinetic of aggregation. This phenomena was noticed to be more evident with the samples containing 5 (w/w)% of MMT. This aggregation is the first step in gelation, which prevents the spinning of these solutions and fibers formation.

To avoid solution gelification or polymer precipitation, fibers were obtained by spinning solution with polymer concentration just below Cp′.

Table 1 summarizes the mechanical characteristics of PBA and PBA/MMT fibers, obtained from solution of PBA in DMAc/LiCl ($C_p = 6.5\%$ (w/w)) with 2.6–5% (w/w) of MMT using two different draw ratios.

The fibers appear homogeneous without any morphological differences compared to fibers obtained from neat PBA. PBA/2.6% (w/w) MMT nano-composite fibers, sample 3–4, present smaller diameters than PBA fibers at the same spinning condition. This phenomena is probably due to a smaller die swell of the nano filled solution than the one without MMT, due to the interactions between polymer and nanofiller, that changes the viscoelastic characteristic of the solutions. So this means that MMT nanofillers are homogeneously dispersed in PBA/DMAc-LiCl solution and the dope flows without occluding the 100 μm spinnerette hole. For greater MMT concentration no differences of diameter between

Table 1.
Mechanical properties of PBA fibers and PBA/MMT nanocomposite fibers.

Samples	MMT	Draw ratio	Diameter	E	σ_b	ε
	(w/w)%		μm	GPa	Mpa	%
1	0	1	40	8.3	104	9
2	0	2	24	21.5	364	6
3	2.6	1	29	18.1	405	8
4	2.6	2	19	26.2	525	12
5	5	1	38	8.3	101	5
6	5	2	23	24.8	388	4

neat PBA fibers and PBA/MMT nanocomposite fibers was observed, this could be correlated to an aggregation of the particles and an inhomogeneous dispersion.

The tensile strength and elongation at break of fibers with 2.6wt% MMT, samples 3 and 4, showed greater values with respect to those of pure PBA. These results are due to MMT presence in the fibers which may interact with PBA matrix, and improve mechanical properties.An increase in modulus and breaking strength of about 78% and 290% for samples without draw ratio was observed. While samples drawn twice show a lower increase of about 22% for the modulus and 44% for the breaking strength. With regards to elongation at break, PBA/MMT fibers showed a similar tendency as the tensile strength with MMT content. The elongation break for PBA/MMT nano-composites fibers increases with V_l/V_f, going from 8 to 12% against a decrease from 9 to 6% for neat PBA fibers. The increase in the tensile strength and elongation at break could be caused by the interfacial interaction between MMT and PBA matrix due to physical and chemical effects. Moreover the large amount of interface between MMT sheets and PBA could effectively reduce the formation of a shear zone and a layer structure of MMT so as to stop the development from the shear zone to cracks,[20] and then leading to the increasing in strength and ductility.

The tensile strength and elongation properties of the fibers decreased with the increase of MMT content up to 5% (w/w), samples 5 and 6, this might be attributed to MMT agglomerates increase in PBA matrix.

Furthermore we obtained an useful insight into the nature of polymer-clay nano-composites from TGA. Figure 4 compares the thermal stability of PBA/MMT and PBA fibers. The presence of MMT influences the thermal stability of fibers in oxidant ambient. At the temperature of about 320 °C, PBA degradation begins to appear while for PBA-MMT the degradation starts at about 600 °C. This can be attributed to the enhancement of interaction between the polyamide matrix and MMT particles, which limited the segmental movement of the polyamide. The thermal gravimetrical analysis of MMT-30B organophilic clay reveals a decrease of weight at temperature below 350 °C related to the thermal decomposition of the alkylammonioum ions, while MMT-Na^+ Clay do not show any degradation until 500–700 °C where the dehydroxylation of the aluminosilicate is observed.[17] The absence for our samples of weight decreasing due to the presence of alkylammonioum ions it is a further result that confirms the modification of MMT-30B clay in MMT-Li^+ during the solvent treatment.

X-Ray diffraction patterns of PBA/MMT nanocomposite fibers and MMT showed some differences. A shift towards low value of 2θ of diffraction peaks is observed, while the content of MMT

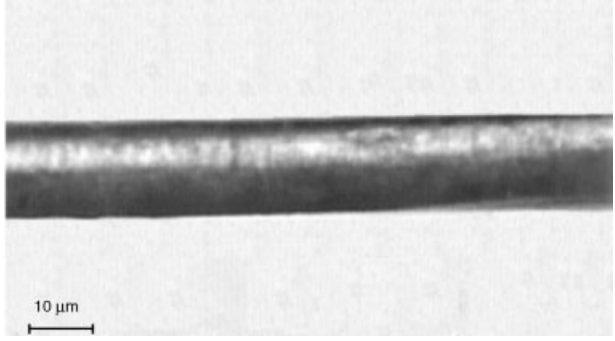

Figure 4.
Photographs at the optical microscopy of PBA/2.6%(w/w) MMT nanocomposite fibers (sample 4; Table 1).

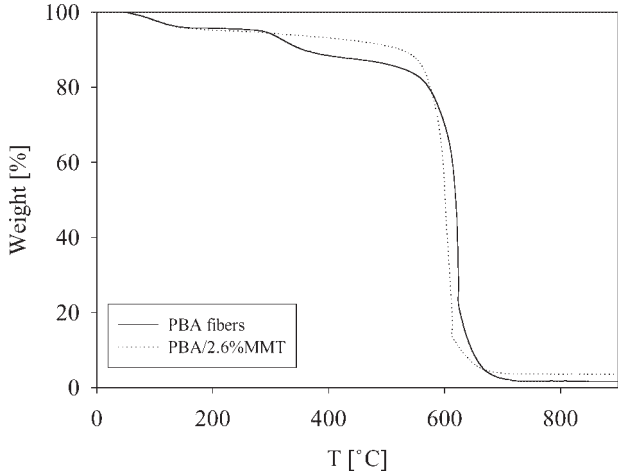

Figure 5.
TGA curves of PBA fibers [solid line] and PBA/2.6%MMT fibers [dotted line].

decreases. However diffraction peaks become weaker, decreasing clays' content, it should be noted that PBA/2.6%(w/w) MMT fibers show a greater value of $d_{(001)}$ than those of MMT one: 1.61 nm against 1.21 nm for MMT treated in DMAc/LiCl.

TEM micrographs (Figure 6) showed that thickly stacked structures are present in fibers' section separated into thinner ones by nano-composite preparation processes. The light grey areas refers to PBA matrix, while the dark areas shows MMT unexfoliated stacks of about some tens of nm in thickness and in length. TEM micrographs showed that layers expansion varies. Smaller expansion predominately occurs in the interior, whereas layer expansion and individual layers are observed near the exterior of stacks.

It was possible to measure the thickness of the layers with an image analysis program, noticing that there was a large and asymmetric distribution of the layers' thickness. The asymmetry was mainly

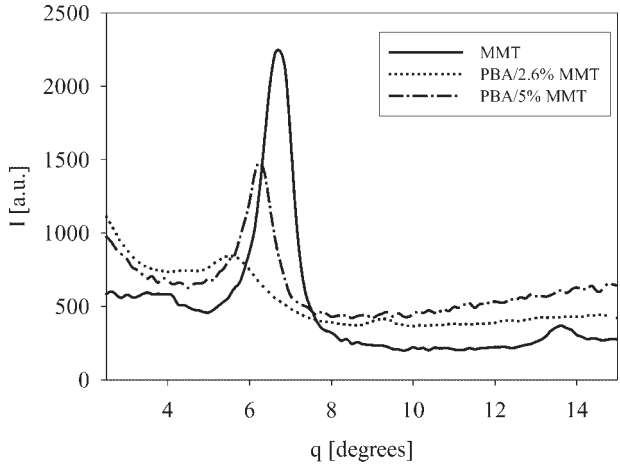

Figure 6.
X-Ray diffraction patterns of MMT [solid line], PBA/5%(w/w) MMT fibers [dotted line], PBA/2.6%(w/w) MMT fibes [dashed line].

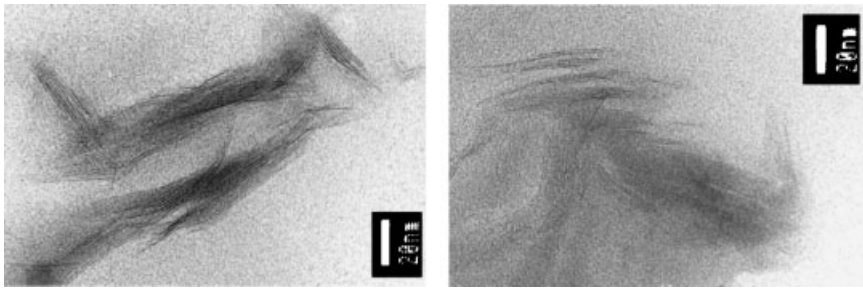

Figure 7.
TEM-Microphotographs of PBA/2.6%MMT fibers.

towards the bigger size: more than 15% of the layers' thickness was above 3 nm for PBA/2.6% (w/w) MMT nanocomposite fibers. These data are consistent with the results of WAXD and they suggest that partially intercalated PBA/MMT nanocomposites fibers have been prepared. Furthermore the intercalation process was more evident decreasing clays' content.

Conclusion

It was possible to prepare PBA nanocomposite fibers with different content of MMT from DMAc/3%(w/w) LiCl solution by a wet spinning line and with different spinning conditions. MMT in PBA/DMAc-LiCl solution does not interfere with the anisotropic phase. The prepared PBA nanocomposite fibers appear homogeneous and for PBA/2.6% (w/w) MMT not only do MMT stacks appear intercalated, but they also disperse almost regularly along and across the fibers' sections. The mechanical properties of these nanocomposite fibers show greater values than those of neat PBA: Young's modulus and breaking strength increase with speed take up. Working with solution at C_p very close to C'_p, MMT could induce an anisotropic phase under shear in the wet spinning line, as it was proved for semi-rigid polymers[21] and this phenomena generates fibers with increased mechanical properties. Furthermore, degradation phenomena in oxidant ambient on PBA/MMT

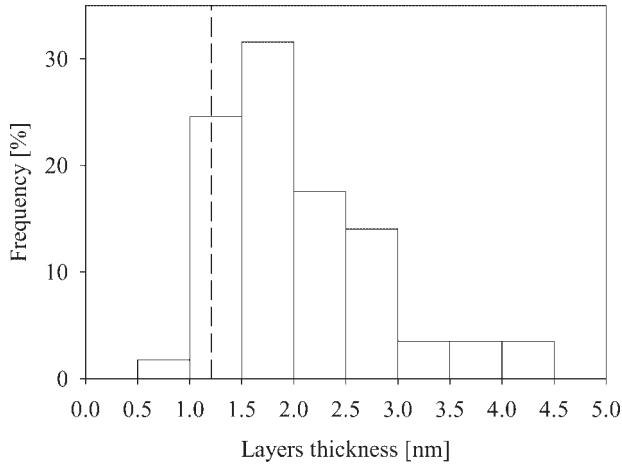

Figure 8.
Distribution of the frequency of layers thickness of PBA/2.6%(w/w) MMT nanocomposite fibers, (Sample 4; Table 1) compared to layers thickness of MMT treated in DMAc/LiCl (dashed line).

fibers are prevented, giving better thermal stability to nanocomposite fibers.

Acknowledgements: The authors wish to thank Mr. Mario Traverso for his helpful work on wet-spinning line.

[1] T. J. Pinnavaia, G. W. Beall, "Polymer-Clay nanocomposites". J. Wiley and Sons, New York, 2002.
[2] M. Alexandre, P. Dubois, *Mater. Sci. and Eng.28* **2000**, *28*, 1.
[3] E. Reynauld, C. Gauthier, J. Perez, *Rev. Metall./Cah. Inf. Tech.* **1999**, *96*, 169.
[4] G. Lagaly, *Applied Clay Science* **1999**, *15*, 1.
[5] C. Oriakhi, *Chem. Br.* **1998**, *34*, 59.
[6] J. Jordan, K. I. Jacob, R. Tannenbaum, M. A. Sharaf, I. Jasiuk, *Mater. Sci. and Eng.* **2005**, *393*, 1.
[7] G. H. Guan, C. C. Li, D. Zhang, *J. Appl. Polym. Sci.* **2005**, *95*, 1443.
[8] E. Giza, H. Ito, T. Kikutani, N. Okui, *Journal of Macromolecular Science Physics* **2000**, *B39*, 545.
[9] H. Fong, W. D. Liu, C. S. Wang, R. A. Vaia, *Polymer* **2002**, *43*, 775.
[10] S. Pavlikova, R. Thomann, P. Reichert, R. Mulhaupt, A. Marcincin, E. Borsig, *Macromolecules* **2004**, *37*, 9076.
[11] S. Y. Yeo, H. J. Lee, S. H. Jeong, *Journal of Materials Science* **2003**, *38*, 2143.
[12] X. Q. Zhang, M. S. Yang, Y. Zhao, S. M. Zhang, X. Dong, X. X. Liu, D. J. Wang, D. F. Xu, *J. Appl. Polym. Sci.* **2004**, *92*, 552.
[13] M. C. Weisenberger, E. A. Grulke, D. Jacques, T. TRantell, R. Andrews, *Journal of Nanoscience and Nanotechnology* **2003**, *3*, 535.
[14] N. Yamazaki, M. Matsumoto, P. Higashi, *J. Polym. Sci.: Polymer Chem. Ed.* **1975**, *13*, 1373.
[15] J. R. Schaefgen, V. S. Foldi, F. M. Logullo, V. H. Good, L. W. Gulrich, F. L. Killian, p. 1–69. American Chemical Society, 1976.
[16] G. Conio, R. Bruzzone, A. Ciferri, E. Bianchi, A. Tealdi, *Polymer Journal* **1987**, *19*, 757.
[17] D. Burgentzléa, J. Duchet, J. F. Gérard, A. Jupin, B. Fillon, *Journal of Colloid and Interface Science* **2004**, *278*, 26.
[18] J. R. Schaefgen, T. I. Bair, J. W. Ballou, S. L. Kwolek, P. W. Morgan, M. Panar, J. Zimmeman, *in* "Ultra-high modulus polymer" I. M. Ward, Ed., Chapter 6. Applied science publishers, London, 1979.
[19] C. Balbi, E. Bianchi, A. Ciferri, A. Tealdi, W. R. Krigbaum, *J. Polym. Sci.: Polymer Physics. Ed.* **1980**, *18*, 2037–2053.
[20] Y. H. Zhang, S. Y. Fu, R. H. Y. Li, L. F. Li, G. T. Li, Q. Yan, *High Tech Lett* **2004**, *5*, 99.
[21] A. Ciferri, B. Valenti, *in* "Ultra-high modulus polymers" I. M. Ward, Ed., Chapter 7. Applied science publishers, London, 1979.

